Influence of the heat transfer field on anomalous lubricant film formation in elastohydrodynamic lubrication conditions

Kazuyuki Yagi (yagik@mech.kyushu-u.ac.jp)
Kyushu University https://orcid.org/0000-0002-2293-0546
Kazuki Nishida
Kyushu University: Kyushu Daigaku
Joichi Suigmura
Kyushu University: Kyushu Daigaku

Research Article

Keywords: elastohydrodynamic lubrication (EHL), lubricant film

Posted Date: May 14th, 2021

DOI: https://doi.org/10.21203/rs.3.rs-500549/v1

Version of Record: A version of this preprint was published at Tribology Letters on August 7th, 2021. See the published version at https://doi.org/10.1007/s11249-021-01492-0.

Abstract

The influence of the heat transfer field on anomalous film formation under elastohydrodynamic lubrication (EHL) conditions was studied. Liquid lubricant film shapes between a transparent disc and steel ball friction pair were investigated by white light optical interferometry. 1-Dodecanol was used as the representative lubricant to develop anomalous film shapes. A sapphire disc and glass disc, which have different thermal conductivities, were used as the transparent bounding surface. The heat transfer field significantly influenced the formation of anomalous film shapes. The anomalous film shapes approximated the shape of a conventional EHL film with increasing ambient temperature. However, a thickened part of the lubricant film remained, although the phase diagram of 1-dodecanol suggested it to be in the liquid state.

Introduction

Elastohydrodynamic lubrication (EHL) has been one of the most important topics in the tribological field for over a century. Pressure develops at the entrance of the contact area and builds up to the order of several gigapascals. A significantly high pressure causes large elastic deformations of the bounding surfaces and an increase in the viscosity of the lubricant, termed as the piezoviscous effect [1]. The film formed in the lubricated area has a specific shape with a flat part around the contact area and a constricted shape at the exit zone [2]. A lubricant film with a thickness of less than 1 μm is greatly sheared under the movement of the bounding surfaces at speeds of several metres per second.

For a better understanding of EHL, both the traction and the film thickness are important information. Traction is generated in the contact area, where a lubricant film of significantly high viscosity is sheared at a high shear rate of the order of 10^6 s^{-1}. A lubricant film under significant shearing force does not exhibit the Newtonian rheological behaviour. Instead, it shows shear thinning, viscoelastic, or elastoplastic behaviour [3–8]. On the contrary, it has been recognised that the film thickness is determined by the flow at the entrance with a great geometrical convergent shape [9]. The formed film has a specific shape; it is flat around the central area and constricted at the exit zone [2]. Representative formulas have been suggested for the film thickness at the centre and minimum film thickness for conveniently designing the lubricated area [10]. A fast numerical simulation algorithm has also been developed for solving the EHL problems [11].

Further, the influence of the rheological characteristics of the lubricant within the lubricated area on the film formation has attracted increasing interest over the last two decades. Significant variations in the film shape were identified under rolling/sliding conditions [12–20] and opposite sliding conditions at a zero entrainment speed [21, 22], and in the cases of high-viscosity oil [23] and liquids with a clear melting point [24–30]. Variations in the film shape under rolling/sliding conditions [12–20] and opposite sliding conditions [21, 22] were concluded to arise from the viscosity wedge action [29], whereas the film shape variations in the cases of high-viscosity oils [23] and liquids with a clear melting point [24–30] remain to be fully understood.

Herein, we present the appearance of anomalous film shapes in the case of a liquid with a clear melting point [24–30]. Anomalous film shapes were discovered at the point contact area between a glass disc and a steel ball lubricated with a fatty alcohol, 1-dodecanol [24–27]. Under pure rolling conditions, the film was found to have the conventional shape [2]. The shape of the film however changed, resulting in a gradual increase in the film thickness around the central zone with increasing slide-to-roll ratio. At high slide-to-roll ratios, the thickened part moved towards the entrance, and then a thinner part of the film dominated. The film shape depended on the sign of the slide-to-roll ratio at high slide-to-roll ratios; the thickened part tended to move towards the entrance at higher steel ball speeds, whereas it tended to remain in the lubricated area at higher glass disc speed. In ensuing studies, other fatty alcohols [26], an acid, an amine, a chloride, and various alkanes [28] were found to adopt the same film shape as 1-dodecanol. Furthermore, the maximum traction coefficient was observed at a low slide-to-roll ratio, and the value decreased gradually with increasing slide-to-roll ratio for 1-dodecanol and other liquids that developed anomalous film shapes. In contrast, liquids developing the conventional film shape exhibited a gradual increase in the traction coefficient with increasing slide-to-roll ratio [28]. The shear rate of the maximum traction coefficient for liquids developing anomalous film shapes ranged from 10^5 to 10^7 s^{-1}, which is of the same order as those of traction fluids [29]. The shear rate depends on the liquid type; for example, the shear rates for *n*-tetradecane and *n*-hexadecane (alkanes) are ~ 2.0×10^6 s^{-1}, while that of 1-dodecanol (an alcohol) is ~ 4.0×10^5 s^{-1}. Reddyhoff et al. [30] focused on the transition of the traction behaviour of 1-dodecanol with pressure and ambient temperature.

The anomalous film formation in the case of liquids with a clear melting point [24–30] has been attributed to the solidification of the lubricant. In a previous study [25], a small temperature rise of ~ 30°C was estimated using a simple temperature formula based on the assumption of semi-infinite bodies. However, the heat generated in the film influences the formation of anomalous film shapes, because the possibility can be predicted based on the trend of the traction coefficient with increasing slide-to-roll ratio and a significant difference in the film shapes at positive and negative slide-to-roll ratios at the glass–steel contact. Therefore, in the current study, we focused on the influence of the heat transfer field on the film formation. White light optical interferograms of the film formed at the point contact area between a transparent disc (glass or sapphire) and steel ball were captured. Sapphire and glass with different thermal conductivities were used as one of the surface materials to change the heat transfer field of the friction surfaces. The formation of the anomalous film shapes was investigated by changing the material of one of the bounding surfaces, sliding conditions, and ambient temperature.

Experimental Procedure

Tests were conducted using a ball-on-disc type test rig, as reported previously [28, 29], to study the variations in the lubricant film thickness and traction. Fig. 1 shows a schematic of the test rig. A point contact area was created between a rotating transparent disc (diameter: 80 mm; thickness: 5 mm) and a rotating steel ball (diameter: 25.4 mm). SUJ2, which is equivalent to AISI52100, was used as the steel substrate. The rotational speeds of the disc and ball are independently controlled using AC servo motors

to set desired slide-to-roll ratios. The ball and disc are placed in a chamber containing the lubricant. The temperature of the chamber is controlled using a heating system consisting of heat pipes, a thermistor, and a controller. The lubricant is supplied to the contact area by ball rotation. An optical microscope is installed above the test rig to measure the film thickness via white light optical interferometry. White light from the microscope is illuminated onto the contact area, and the reflected light is captured by a digital camera attached to the microscope. A thin chromium layer was deposited on the contact side of the disc surface to increase the contrast of the optical interferograms between the transparent disc surface and steel ball.

A BK7 glass disc or a sapphire disc was used as the transparent material. Both these materials are transparent to visible light, but have different thermal conductivities. Table 1 lists the properties of the two discs and steel ball counterpart. A fatty alcohol, 1-dodecanol, was used as the representative liquid lubricant that develops anomalous film shapes, as demonstrated in previous studies [24–28].

The slide-to-roll ratio, S is defined as follows:

$$S = \frac{u_b - u_d}{u_m}. \quad (1)$$

where u_b is the ball speed and u_d is the disc speed. The entrainment speed, u_m is defined as $u_m = (u_b + u_d)/2$. When the ball speed is higher than the disc speed, S is positive, and when the ball speed is lower than the disc speed, S is negative.

Table 1
Properties of steel, glass, and sapphire

Properties	Steel	Glass	Sapphire
Young's modulus (GPa)	210	81	365
Poisson's ratio	0.300	0.208	0.2
Density (kg/m^3)	7850	2510	3980
Thermal conductivity (W/mK)	46.00	1.11	27.00
Specific heat (J/kg K)	470	840	577

The phase diagram of 1-dodecanol was constructed using a diamond anvil cell device. Figure 2 shows a schematic of the diamond anvil cell device. A gasket of stainless steel SUS304 (thickness: 0.5 mm) with a 0.6 mm diameter hole was sandwiched between the diamond anvils with a currete diameter of 1.2 mm. A small amount of the lubricant, 1-dodecanol, and a piece of ruby were introduced into the hole. A hydraulic pressure was applied to the lubricant by tightening a screw attached to the device. The temperature of the device was controlled using a heating system consisting of heat pipes, a K-type

thermocouple, and a controller. The pressure was calculated on the basis of the fluorescence of ruby [31]. The phase state of the lubricant was observed with a transmission optical microscope. The phase state of the lubricant was confirmed from the appearance of the lubricant crystal grains in the visible images.

Results

Figure 3 Optical interferograms of the lubricant film at the glass–steel contact at different slide-to-roll ratios under the applied load of 40 N (the maximum Hertzian pressure and Hertzian radius were 0.57 GPa and 183 μm, respectively) and ambient temperature of 30°C.

Figure 5 shows the variation in the traction coefficient with the slide-to-roll ratio. The traction coefficient had the maximum value at low S, and then it decreased monotonically with increasing S. The maximum values of the traction coefficient at the sapphire–steel contact were smaller than those at the glass–steel contact. However, the traction coefficient at the sapphire–steel contact was greater than that at the glass–steel contacts at greater S, because of the marginal decrease in the traction coefficient with S at the sapphire–steel contact.

Figure 6 shows the optical interferograms recorded to study the film thickness variation at the glass–steel contact at the ambient temperatures of 30, 50, and 70°C under different positive S values, while Fig. 7 shows the variation under the same conditions under negative S values. Figure 8 shows the variation in the traction coefficient under the same operating conditions as those of Fig. 6 (i.e., at different positive S values). The tests were conducted to investigate the film formation behaviour of 1-dodecanol in the liquid state. The phase state of 1-dodecanol was confirmed from the maximum Hertzian pressure, ambient temperature, and its phase diagram. Both the film thickness and the shape changed with increasing ambient temperature. Under pure rolling conditions, the film thickness decreased to less than 70 nm at 70°C because of the decrease in the viscosity of 1-dodecanol. However, the thicker part of the film around the central zone remained even at the ambient temperature of 70°C, when 1-dodecanol appeared to be in the liquid state. The thickened part of the film showed a greater tendency to remain at a higher negative S than at positive S at the ambient temperature of 30°C, whereas the trend was reversed at the ambient temperature of 70°C. The traction coefficient decreased with increasing ambient temperature. The trend of the traction coefficient with respect to S at 70°C was different from the trends at 30 and 50°C; the traction coefficient increased gradually with increasing S at 70°C.

Figure 8 Variations in the traction coefficient at the glass–steel contact under the applied load of 20 N (the maximum Hertzian pressure was 0.45 GPa) at different slide-to-roll ratios and different ambient temperatures of 30, 50, and 70°C. The operating conditions were the same as those of Fig. 6.

Discussion

The tests revealed that the anomalous film shape of the liquid lubricant depends on the heat transfer conditions, such as the material of the bounding surfaces and ambient temperature. At the glass–steel

contact, the shape/thickness of the film depended on the sign of *S*; a thin film part expanded over the lubricated area at a high positive *S* value with a higher ball speed, whereas a thick part of the film remained at a high negative *S* value with a lower ball speed, as shown in Fig. 3. In contrast, at the sapphire–steel contact, the shape/thickness of the film was almost symmetrical with respect to the sign of *S*; a thick film existed between the inlet zone and central zone, and the film was slightly thinner at positive *S* than at negative *S*, as shown in Fig. 4. These differences in the film formation behaviours can be attributed to the different thermal conductivities of the glass and sapphire discs. The thermal conductivity of glass is significantly lower than that of sapphire (Table 1). It is well-recognised that the thermal properties of bounding surfaces greatly influence the film formation characteristics. One of the representative findings on the influence of the thermal properties of the bounding surfaces is a dimple discovered by Kaneta et al. [19, 20], which appeared under simple sliding contact conditions between a moving glass disc and stationary steel ball counterpart, but was not observed when the steel surface was slid against the stationary glass disc. The thick film formation in the current study is the opposite trend to the dimpling phenomenon reported by Kaneta et al. [19, 20]. Further studies are necessary to clearly comprehend how the differences in the thermal properties of the bounding surfaces influence the lubricant film formation.

A solid-like behaviour was indicated by the variations in the traction coefficient as well as the film thickness/shape. The maximum traction coefficient at a low *S*, and a gradual decrease in the traction coefficient with increasing *S* were observed, as shown in Fig. 5. This is a typical trend observed in the cases of traction oils [6–8], which were speculated to behave like elastoplastic materials. Further, a decrease in the traction coefficient with increasing ambient temperature, which is shown in Fig. 8, has also been observed for traction fluids [6–8]. The gradual increase in the traction coefficient with *S* at the ambient temperature of 70°C is different from the trend observed at the other lower ambient temperatures. The trend observed at 70°C is similar to the trends of ethylene glycol and glycerol, which develop conventional film shapes [28, 29]. However, a thickened part of the film appeared around the central zone at a high *S*, as shown in Fig. 6.

Figures 10 and 11 show the visible images of 1-dodecanol in the liquid and solid states, and the phase diagram of 1-dodecanol. The phase states at the contact area, which were estimated from the ambient temperature and maximum Hertzian pressure under the current operating conditions, are plotted in Fig. 11. At the ambient temperature of 70°C, 1-dodecanol exists in the liquid state, as shown in Fig. 11. This fatty alcohol may solidify in the contact area, although the phase diagram indicates a liquid state under static conditions. There are two possibilities for the increase in the melting temperature of 1-dodecanol in the lubricated area. The first is the alignment of the lubricant molecules along the sliding direction under high shear rates. 1-Dodecanol has a simple linear chain structure, and thus tends to align along the sliding direction. The second possibility is the increase in the melting point of a thin film confined between two solid surfaces. It has been reported that the melting point of a film on a solid surface increases for a monolayer of 1-dodecanol [33–36]. This might be a possibility, although the film is considerably thicker in the current study. These two phenomena suppress the movement of the

lubricant molecules; these are related to the adsorption of additives on surfaces as well as the solidification phenomenon described in the current study.

The current parametric study under varying slide-to-roll ratio, surface material, and ambient temperature revealed the solid-like behaviour of the film formation and traction. Additionally, the current study provides key guidelines for further studies on this topic. Further studies on the mechanisms of the anomalous film formation can aid understand the other aspects of boundary lubrication as well as EHL and hydrodynamic lubrication.

Conclusions

In this study, the film formation behaviours and anomalous film shapes of a long-chain alcohol, 1-dodecanol, were investigated. Parametric experiments were conducted with a focus on the influence of the heat transfer conditions. BK7 glass and sapphire, which have significantly different thermal conductivities, were tested as one of the contact pairs. Optical interferograms of the film thickness were captured by changing the slide-to-roll ratio and ambient temperature. The phase diagram of 1-dodecanol was used to determine the phase state of the lubricant in the contact area. The following results were obtained:

When a sapphire disc was used as one of the contact surfaces, the shape and thickness of the anomalous films were almost symmetrical with respect to the sign of the side-to-roll ratio. In contrast, when a glass disc was used, the films were not symmetrical. The traction coefficient according to the slide-to-roll ratio showed a trend similar to that of a traction oil; it had a maximum value at a low slide-to-roll ratio, and then decreased gradually with increasing slide-to-roll ratio. The maximum traction coefficient in the case of the sapphire disc was slightly lower than that for the glass disc. The gradient of the decrease in the traction coefficient at high slide-to-roll ratios for the sapphire disc was smaller than that for the glass disc. Consequently, the trend of the traction coefficient between the sapphire disc and glass disc was reversed at high slide-to-roll ratios.

The film thickness and the fraction of the thickened part of the anomalous film decreased with increasing ambient temperature. The trend of the traction coefficient changed from that of a traction fluid to that of a viscous fluid; the traction coefficient increased monotonically with increasing slide-to-roll ratio. However, a small thickened part of the film remained around the central zone, although the lubricant was speculated to be in the liquid state based on the maximum Hertzian pressure and ambient temperature.

Declarations

Acknowledgement

This work was supported by JSPS KAKENHI Grant number 21686016, Grant-in-Aid for Young Scientists (A).

References

1. Bridgman, P.W.: Viscosities to 30,000 kg/cm^2. Proc. Amer. Acad. **77**, 117–128 (1949).
2. Gohar, R., Cameron A.: Optical measurement of oil film thickness under elastohydrodynamic lubrication. Nature **200**, 458–459 (1963).
3. Smith, F.W.: Lubricant behavior in concentrated contact systems- the castor oil-steel system. Wear **2**, 250–263 (1958).
4. Smith, F.W.: Lubricant behavior in concentrated contact-some rheological problems. ASLE Trans. **3**, 18–25 (1960).
5. Smith, F.W.: The effect of temperature in concentrated contact lubrication. ASLE Trans. **5**, 142–148 (1962).
6. Johnson, K.L., Tevaarwerk, J.L.: Shear behaviour of elastohydrodynamic oil films. Proc. Roy. Soc. Lond., Ser. A **356**, 215–236 (1977).
7. Evans, C.R., Johnson, K.L.: The rheological properties of elastohydrodynamic contacts. Proc. Inst. Mech. Engrs. **200**, 303–312 (1986).
8. Evans, C.R., Johnson, K.L.: Regimes of traction in elastohydrodynamic lubrication. Proc. Inst. Mech. Engrs. **200**, 313–324 (1986).
9. Grubin, A.N.: Investigation of the contact of machine components. Central Scientific Research Institute for Technology and Mechanical Engineers, Moscow (DSIR translation 337) (Ed. Ketova Kh.F.) 30, (1949).
10. Hamrock, B.J., Dowson, D.: Ball bearing lubrication: The elastohydrodynamics of elliptical contacts. John Wiley & Sons, New York (1981).
11. Venner, C.H., Lubrecht, A.A.: Multi-level methods in lubrication. Elsevier Science B.V., Amsterdam (2000).
12. Foord, C.A., Wedeven, L.D., Westlake, F.J., Cameron, A.: Optical elastohydrodynamics. Proc. Inst. Mech. Engrs. Part 1 **184**, 487–505 (1969–70).
13. Nagaraj, H.S., Sanborn, D.M., Winer, W.O.: Surface temperature measurements in rolling and sliding EHD contacts. ASLE Trans. **22**, 277–285 (1979).
14. Wedeven, L.D.: Discussion to Najaraj's paper. ASLE Trans. **22**, 285 (1979).
15. Sanborn, D.M., Winer, W.O.: Fluid rheological effects in sliding elastohydrodynamic point contacts with transient loading: 1-film thickness. Trans. ASME J. Lubr. Technol. **93**, 262–271 (1971).
16. Sadeghi, F., Sui, P.C.: Thermal elastohydrodynamic lubrication of rolling/sliding contacts. Trans. ASME J. Tribol. **112**, 189–195 (1990).
17. Yagi, K., Kyogoku, K., Nakahara, T.: Temperature measurements of both sliding surfaces and estimation of temperature profile across film thickness under EHL conditions. J. Jpn. Soc. Tribol. **47**(4), 321–328 (2002).

18. Yagi, K., Kyogoku, K., Nakahara, T.: Experimental investigation of effects of slip ratio on elastohydrodynamic lubrication film related to temperature distribution in oil films. Proc. Inst. Mech. Eng. Part J **220**(4), 353–363 (2005).
19. Kaneta, M., Nishikawa, H., Kameishi, K., Sakai, T, Ohno, N.: Effects of elastic moduli of contact surfaces in elastohydrodynamic lubrication. Trans. ASME J. Tribol. **114**, 75–80 (1992).
20. Kaneta, M., Nishikawa, H., Kanada, T., Matsuda, K.: Abnormal phenomena appearing in EHL contacts. Trans. ASME J. Tribol. **118**, 886–892 (1996).
21. Yagi, K., Kyogoku, K., Nakahara, T.: Mechanism of dimple formation under elastohydrodynamic conditions. In: Dowson, D., Priest, M., Dalmaz, G., Lubrecht, A.A., editors. Proceedings of the 29th Leeds-Lyon Symposium on Tribology, Elsevier B. V., Amsterdam, 111–120 (2003).
22. Yagi, K., Kyogoku, K., Nakahara, T.: Relationship between temperature distribution in EHL film and dimple formation. Trans. ASME J. Tribol. **127**(3), 658–665 (2005).
23. Chiu, Y.P., Sibley, L.B.: Contact shape and non-Newtonian effects in elastohydrodynamic point contacts. Lubr. Eng. **28**, 48–60 (1972).
24. Yagi, K., Vergne, P.: Film thickness changes in EHD sliding contacts lubricated by a fatty alcohol. Tribology Online **1**, 5–8 (2006).
25. Yagi, K., Vergne, P.: Abnormal film shapes in sliding elastohydrodynamic contacts lubricated by fatty alcohols. Proc. Inst. Mech. Eng. Part J **221**, 287–300 (2007).
26. Yagi, K., Sugimura, J., Vergne, P.: Rheological response of fatty alcohols in sliding elastohydrodynamic contacts. Tribol. Int. **49**(May), 58–66 (2012).
27. Wang, P., Reddyhoff, T.: Wall slip in an EHL contact lubricated with 1-dodecanol. Tribol. Int. **113**, 197–205 (2017).
28. Yagi, K., Nishida, K., Sugimura, J.: Relationship between molecular structure of lubricant and appearance of anomalous film shapes in elastohydrodynamic lubrication conditions. Tribol. Int. **152**, 106574 (2020).
29. Yagi, K., Nishida, K., Sugimura, J.: Traction behaviour of elastohydrodynamic lubrication films with anomalous shapes. Proc. Inst. Mech. Eng. Part J accepted.
30. Reddyhoff, T., Ewen, J.P., Deshpande, P., Frogley, M.D., Welch, M.D., Montgomery, W.: Macroscale superlubricity and polymorphism of long-chain *n*-alcohols. ACS Appl. Mater. Interfaces **13**, 9239–9251 (2021).
31. Piermarini, G.J., Block, S., Barnett, J.D., Forman, R.A.: Calibration of the pressure dependence of the R1 ruby fluorescence line to 195 kbar. Journal of Applied Physics **46**, 2774–2780 (1975).
32. Cameron, A.: The viscosity wedge. ASLE Trans. **1**, 248–253 (1958).
33. Findenegg, G.H.: Order-disorder transitions at the liquid/solid interface. Volumetric behaviour of primary aliphatic alcohols near the graphon surface. J. Chem. Soc. Faraday Trans. 1 **68**, 1799–1806 (1972).

34. Findenegg, G.H.: Ordered layers of aliphatic alcohols and carboxylic acids at the pure liquid/graphite interface. J. Chem. Soc. Faraday Trans 1 **69**, 1069–1078 (1973).
35. Bien-Vogelsang, U., Findenegg, G.H.: Monolayer phase transitions of dodecanol at the liquid/graphite interface. Colloids and Surfaces **21**, 469–481 (1986).
36. Yeo, Y.H., McGonigal, G.C., Thomson, D.J.: Structural phase transition of a 1-dodecanol monolayer physisorbed at the liquid/graphite interface by scanning tunneling microscopy. Langmuir **9**(3), 649–651 (1993).

Figures

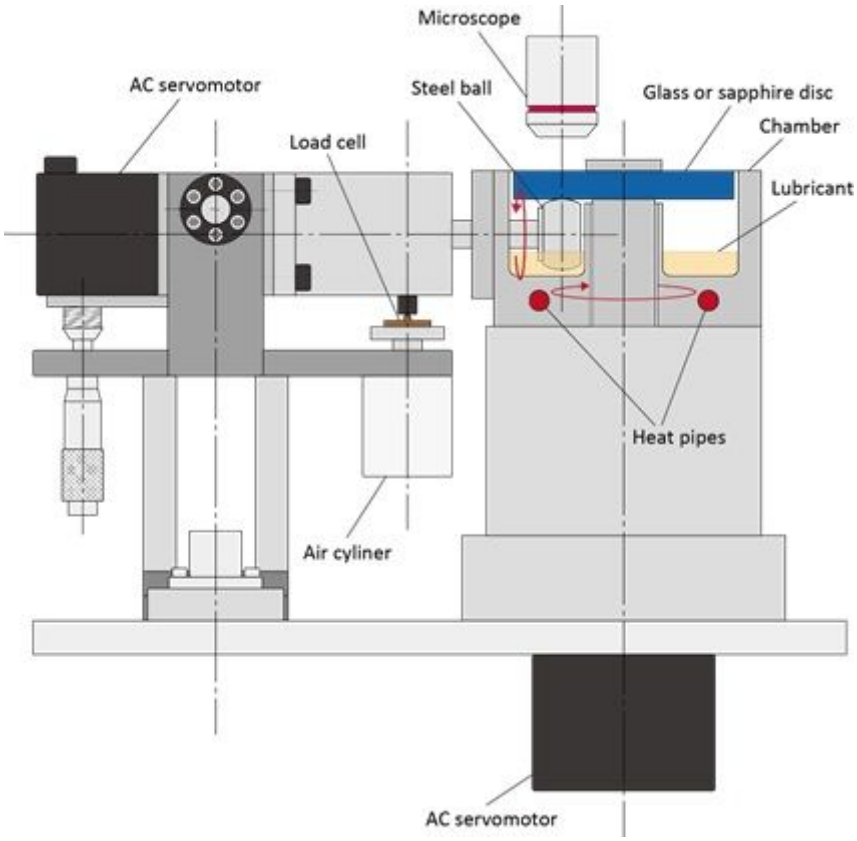

Figure 1

Schematic of the test rig

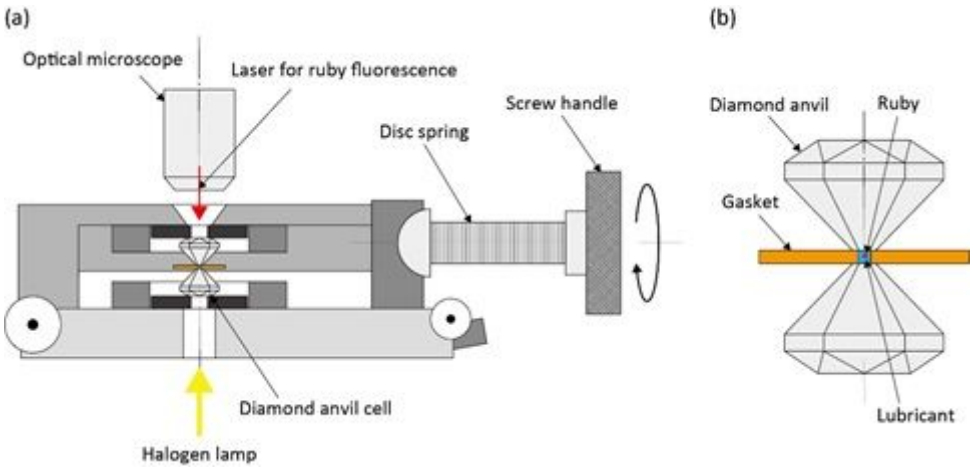

Figure 2

Schematic of the diamond anvil cell device. (a) Full view of the device and (b) enlarged view of the diamond anvil cell

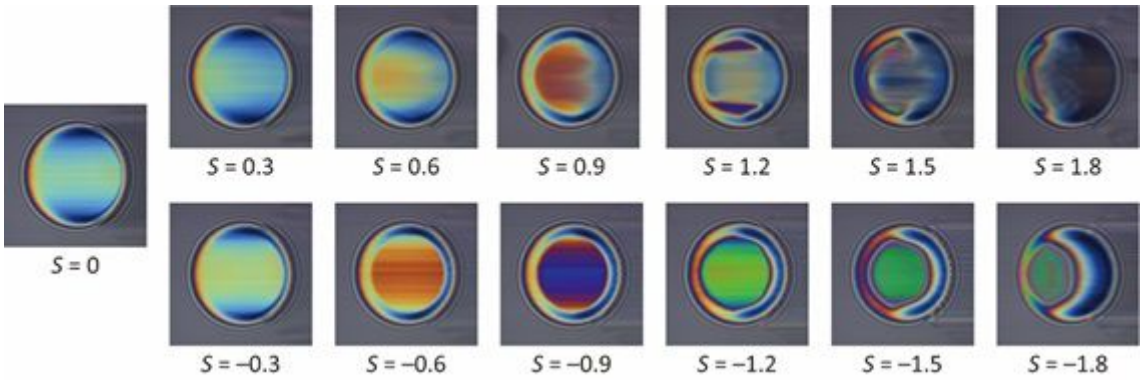

Figure 3

Optical interferograms of the lubricant film at the glass–steel contact at different slide-to-roll ratios under the applied load of 40 N (the maximum Hertzian pressure and Hertzian radius were 0.57 GPa and 183 μm, respectively) and ambient temperature of 30 °C.

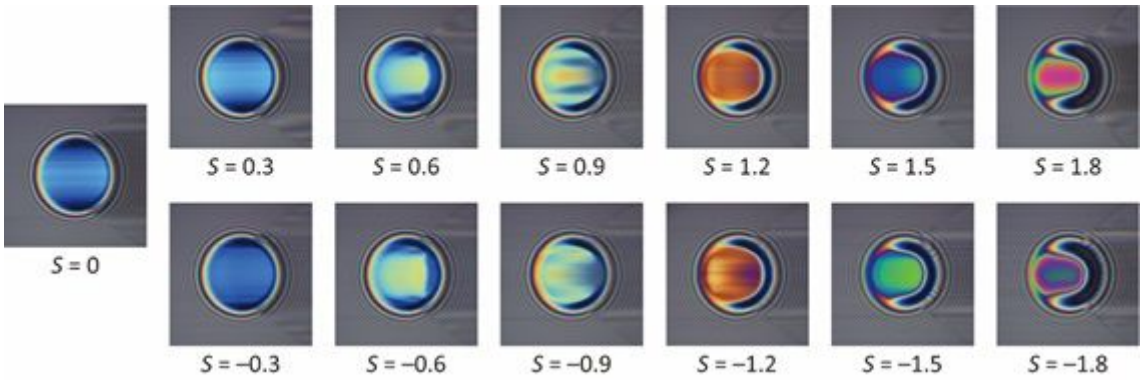

Figure 4

Optical interferograms of the film at the sapphire–steel contact at different slide-to-roll ratios under the applied load of 40 N (the maximum Hertzian pressure and Hertzian radius were 1.00 GPa and 138 μm, respectively) and ambient temperature of 30 °C.

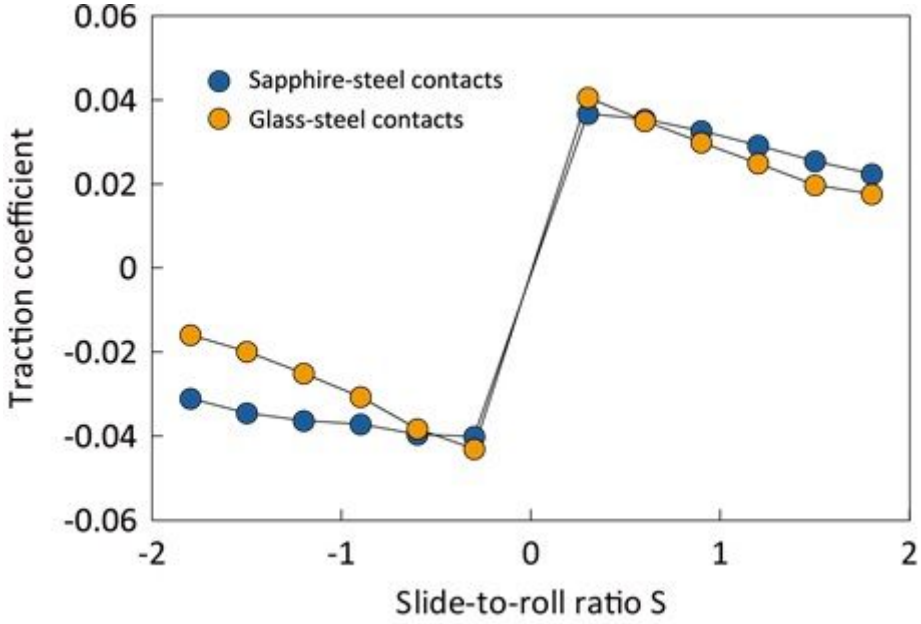

Figure 5

Variations in the traction coefficient with the slide-to-roll ratio under the applied load of 40 N (ambient temperature: 30 °C).

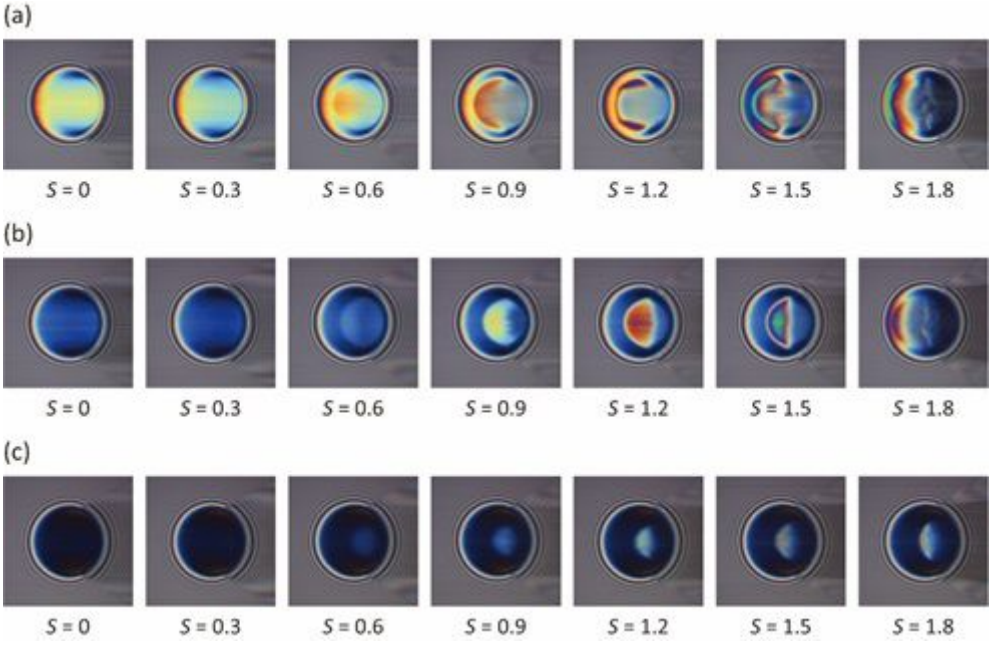

Figure 6

Variations in the optical interferograms of the film at the glass–steel contact under the applied load of 20 N (the maximum Hertzian pressure was 0.45 GPa) at different positive slide-to-roll ratios and ambient temperatures of (a) 30, (b) 50, and (c) 70 °C.

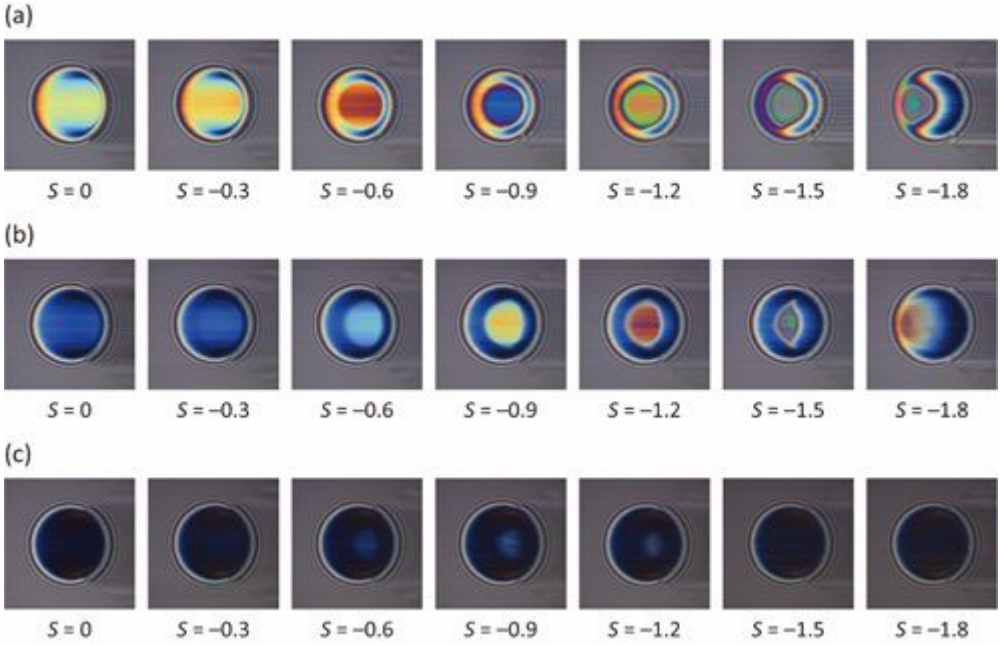

Figure 7

Variations in the optical interferograms of the film thickness at the glass–steel contact under the applied load of 20 N (the maximum Hertzian pressure was 0.45 GPa) at different negative slide-to-roll ratios and ambient temperatures of (a) 30, (b) 50, and (c) 70 °C.

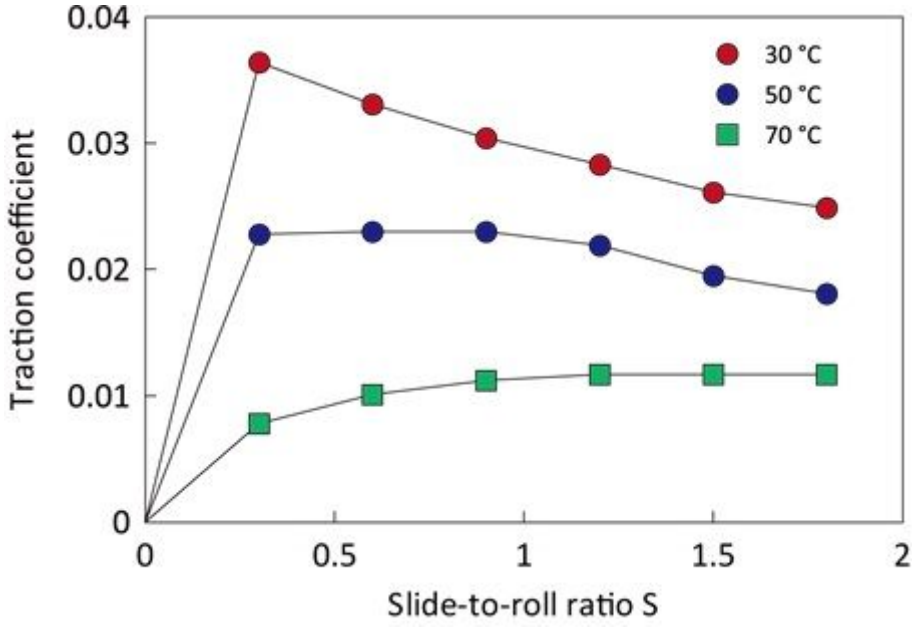

Figure 8

Variations in the traction coefficient at the glass–steel contact under the applied load of 20 N (the maximum Hertzian pressure was 0.45 GPa) at different slide-to-roll ratios and different ambient temperatures of 30, 50, and 70 °C. The operating conditions were the same as those of Fig. 6.

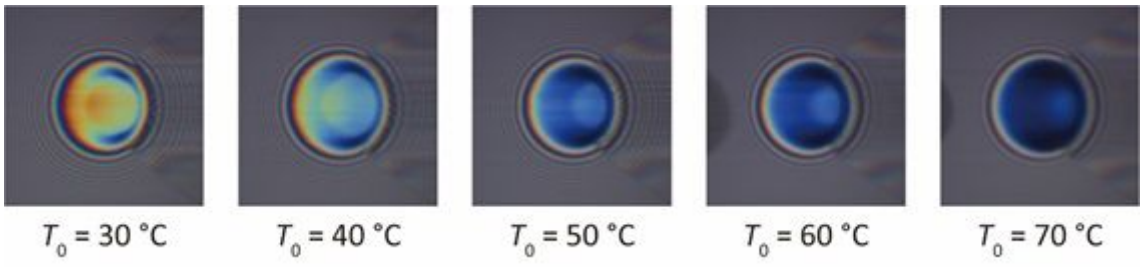

Figure 9

Variations in the optical interferograms of the film thickness at the glass–steel contact under the applied load of 10 N (the maximum Hertzian pressure was 0.36 GPa) and constant slide-to-roll ratio of 0.6 at different ambient temperatures.

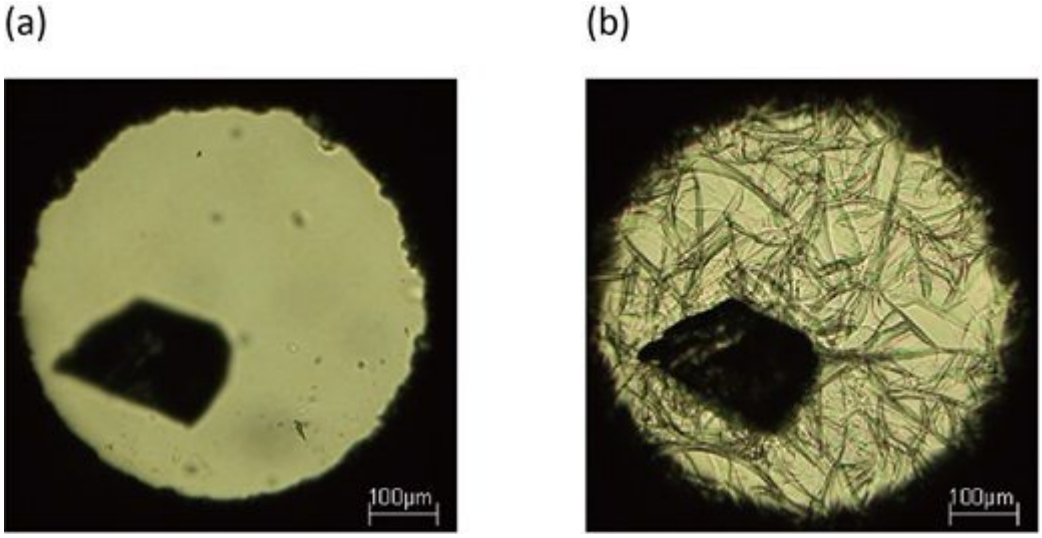

Figure 10

Visible images of 1-dodecanol pressurised by the diamond anvil cell at (a) the atmospheric pressure and (b) at 60 MPa under a constant temperature of 30 °C.

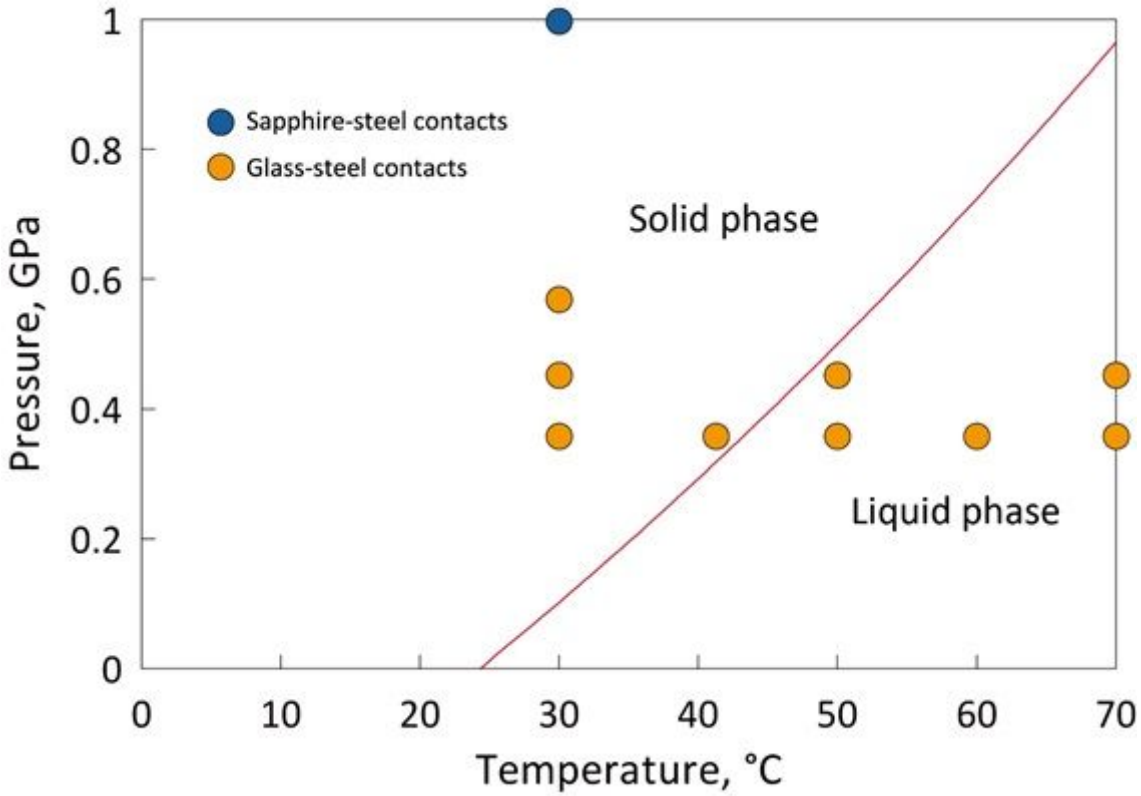

Figure 11

Phase states of the lubricated area, as estimated from the ambient temperature and maximum Hertzian pressure.